LATEST NEWS FROM STOCHASTIC COOLING DEVELOPMENTS FOR THE COLLECTOR RING AT FAIR

R. Hettrich, A. Bardonner, R. Böhm, C. Dimopoulou, C. Peschke, A. Stuhl, S. Wunderlich,
GSI Helmholtzzentrum für Schwerionenforschung, Darmstadt, Germany
F. Caspers, CERN, Geneva, Switzerland and European Scientific Institute (ESI), Archamps, France

Abstract

The CR stochastic cooling system aims at fast 3D cooling of antiprotons, rare isotopes and stable ions. Because of the large apertures and the high electronic gain, damping within the 1-2 GHz band of the unwanted microwave modes propagating through the vacuum chambers is essential. It will be realised within the ultrahigh vacuum using resistively coated ceramic tubes and ferrites. The greatest challenge is increasing the signal to noise ratio for antiproton cooling by means of cryogenic movable (plunging) pickup electrodes, which follow the shrinking beam during cooling and then withdraw fast before the new injection. Linear motor drive units plunge synchronously the pickup electrodes on both sides of the ion beam (horizontal/vertical). Their technical concept is summarized. Their performance has been demonstrated in successive measurements inside testing chambers at GSI. Recent simulations of the critical antiproton cooling with the designed system are shown.

CONCEPT OF PICKUP DRIVES

The concept of linear motor drives for plunging the pickups has been verified. Latest measurements and adjustments have shown that a safe drive concept, with inherent freeing of the aperture in case of an emergency power shutdown, can be built with a single mechanical construction for the all drive orientations.

The springs are the only parts which have to be adjusted for horizontal, vertical top or vertical bottom orientation. Due to the weight of the sliding mass in combination with the vacuum force, springs with three different strengths are needed. In a special test chamber the given forces have been measured and adjusted in order to optimize the dynamic performance. The basic idea is that the drives for the plunging electrodes are outside the vacuum chamber and the movement is decoupled with fatigue endurable bellows. This imposes the full static vacuum force of about 440 N on the drives. To avoid dropping the electrodes onto the beam axis in case of power failure, these vacuum forces are over-compensated with pre-compressed springs. This concept induces an outgoing force on the drives, which increases proportionally to the distance from the outer edge position. The slope of this increase should be as low as possible. The limit is given by the part of the drive length, which can be used for spring pre-compression. In order to get zero total static force at the outer edge position the springs were chosen with maximum length left for pre-compression and spring constants as low as possible. Further, the static forces of the drives including the electrodes and a dummy weight to account planed enhancements have been measured. Then, adequate spacers for precise adjustment of the springs pre-compression have been inserted into the spring enclosure. Thus, for all three orientations a minimum static force configuration has been achieved. The plots for the orientations with the highest and lowest slope of the force versus the 'distance-from-beam-axis' are shown in Fig. 1.

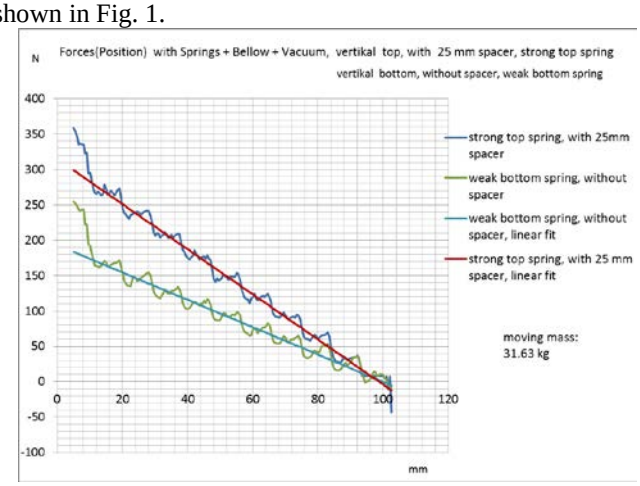

Figure 1: Static forces push out with a ripple from the permanent magnetic field of the motor (current off).

PLUNGING TRAJECTORIES

For the most critical case with the highest slope, the static force could be kept about 100 N below the maximum static force of the motor. This is enough to achieve a 70 mm full scale movement within 120 milliseconds without additional mechanical shock from the inner to the outer edge of the tank in vertical top orientation. This is shown in Fig. 2.

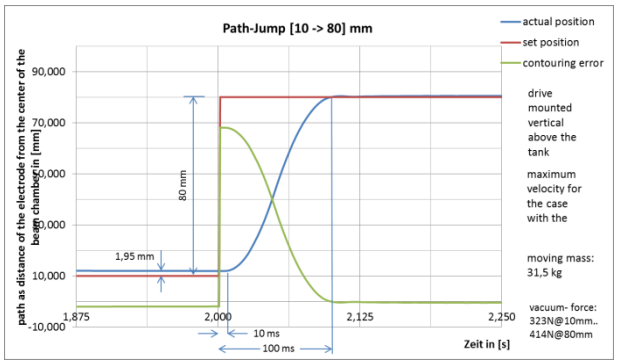

Figure 2: Minimum settling time response (blue) to a full drive distance path jump (red)

To avoid mechanical damage to the extremely sensitive electrodes in a long-term operation, the plunging should work on a jerk-free trajectory. Despite several optimized solutions, we used the profile with the following functions for all practical test sequences. This profile is very common in many other industrial applications and provides a representative mechanical stress situation.

$$s(t) = So + S\,[\frac{t}{T} - \frac{1}{2\pi}\sin\left(\frac{2\pi}{T}\,t\right)],$$

S_o = 10 mm, S = 70 mm, T = {0.2 - 1} s

$$v(t) = \frac{S}{T}\left[1 - \cos\left(\frac{2\pi}{T}\,t\right)\right] = 2\,\frac{S}{T}\,sin^2\left(\frac{\pi}{T}\,t\right),$$

$$a(t) = 2\,\pi\,\frac{S}{T^2}\,\sin\left(\frac{2\pi}{T}\,t\right)$$

This results in a maximum velocity of $2\,\frac{0.07\ m}{0.2\ s} = 0.7\,\frac{m}{s}$ and in a maximum acceleration of $6.28\,\frac{0.07\ m}{0.04\ s^2} = 11\,\frac{m}{s} = 1.12$ g. A typical movement cycle with the given profile is shown in Fig. 3.

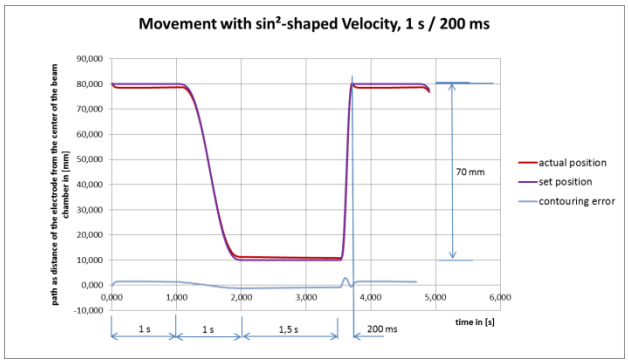

Figure 3: Movement cycle with T = [1s (in), break of 1.5s, 0.2s (out), break of 1s].

HARDWARE CONFIGURATION FOR SYNCHRONOUS DRIVING

To achieve synchronous movement of eight drives inside the tank the following control scheme was applied. Each drive is controlled by a separate industrial drive controller. A common computer with a real-time operating system sends set values to each drive controller, receives the actual values of a programmed control loop in equidistant 1 ms time-steps. The transport of all position values is made by a bus system, called 'EtherCAT'. This system uses the common physical layer of the Ethernet standard, combined with a protocol derived from the Internet Protocol.

In order to achieve sufficient accuracy in positioning the drives, a drive control system with position measurement and feedback of the actual position was used. The drive control scheme is shown in Figure 4.

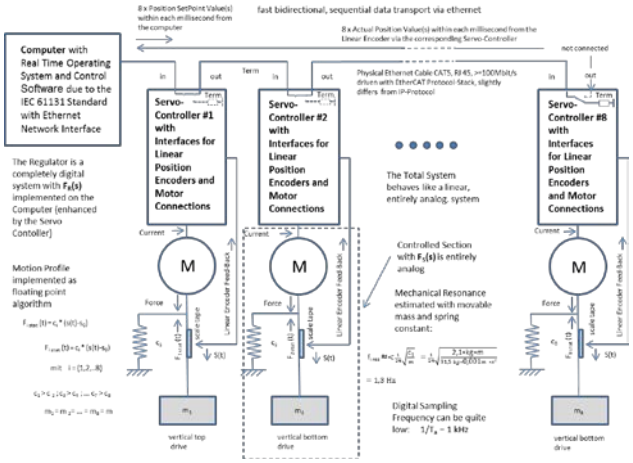

Figure 4: Linear drive control scheme for the CR stochastic cooling pickup tanks.

Unfortunately, the moving mass with the springs for vacuum force compensation is a resonant system with a very low resonance frequency and almost no damping.

$$fres = \frac{1}{2\pi}\sqrt{\frac{c}{m}} = \frac{1}{2\pi}\sqrt{\frac{2.1\ kg\ m}{31.5\ kg\ 0.001\ m\ s^2}} = 1.3\ Hz$$

Such a system cannot be moved as fast and precise as specified above without some kind of damping. The solution was to implement an electronic damping system by a special control loop design. This design overrides the build-in hardware regulator of the industrial drive controller by replacing it by a precompiled PID regulator which is contained in the real-time operating system. Thus, the full parameter set of the regulator can be used to adjust the moving system with sufficient damping. The scheme of the corresponding control loop is shown in Figure 5.

A CONTROL LOOP FOR PRECISION, SPEED AND DAMPING

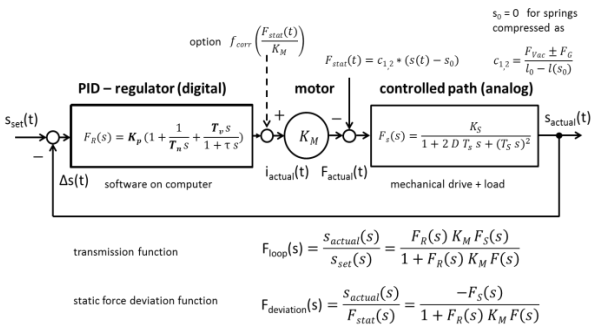

Figure 5: Stable adjustable control loop model with PID regulator and 2-pole path.

The optimal damping is achieved by putting a path jump s(t) = 20 mm·1(t) (for instance) to the control loop. Then, the loop reacts with a damped movement like the one shown in Figure 6.

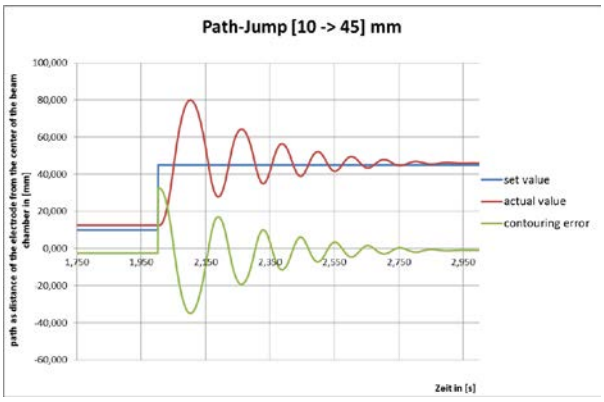

Figure 6: Damped oscillation at the beginning of the control loop adjustment.

After some trials by varying the parameters K_p, T_n and T_v (T is set about 10% of T_v), the expected ringing can be decreased and the movement can be made faster by increasing K_p short below an oscillation. Probably several iterations are necessary until the drives follow the position jump in a rectangular shape. The adjustment procedure behaves similar to the adjustment of a probe of an oscilloscope.

A new adjustment is necessary after each mechanical change concerning the moving mass until the mechanical construction is final. With the right adjustment and the estimated final moving mass of 31.5 kg, the movements shown in the pictures 2 and 3 are possible.

The violet curve on Figure 3 shows the set values in our movement cycle, the red curve shows the corresponding actual values. The comparison reveals a lag of the actual value behind the set value. In the given example, the actual value does not reach the inner or outer target position during the break sequences of 1.0 and 1.5 s, but has a slight slope towards the target position. This slope corresponds to the integration time constant of the regulator (about 3 s in the given adjustment). So, at least 3 s break is needed to reach the target position. The residual position difference of less than 2 mm cannot be zeroed by decreasing the integration time constant, because the needed damping depends on the value of the actual adjustment. The maximum error for the middle-point of two opposite synchronous drives with respect to the beam axis can be estimated by dividing this residual error by two. This results in a deviation of 1 mm for several seconds after reaching the target position. This is fully acceptable for the long cooling times and the broad distributions of the particle beams in the CR.

As an outlook, a correction is achievable: The residual position difference is caused by the static spring forces. These are proportional to the position itself. Therefore, it is possible to develop a correction function, which can be easily subtracted in the numerical path of the loop, if the known force is divided by the motor current-to-force constant K_M=78 N/A. The precise correction function is a weighted response of the loop to the moving profile and the static spring force. A calculation would require a complete model of the not yet designed mechanics in combination with an inverse Laplace transformation of the static force deviation function. The Laplace transform of the loop transfer function and the static force deviation function are shown in Figure 5.

DAMPING OF UNWANTED MICROWAVE MODES

Large-aperture vacuum chambers admit many propagating waveguide modes. The operation with high gain (>130 dB) and a short distance between Palmer pickup and kicker favour self-excitation of the loop. To avoid self-excitation, sufficient microwave damping in the operating frequency band (1-2 GHz and above) is necessary inside the beam chambers. Materials like ferrites and resistively coated ceramics are used for this purpose [1]. They must be acceptable inside ultrahigh vacuum (UHV).

Table 1 summarizes the damping requirements, Figure 8 shows a possible layout of ceramic tubes in the magnet chambers and the space occupied by the beam.

Table 1: Electrical gain and required damping

values for hexagonal quadrupole and sextupole chambers	**slotline pickups to kicker**	**Palmer pickup to kicker**
max. gain	150 dB	133 dB
min. damping	135 dB	130 dB
Σ length of all chambers	19.6 m	12.7 m
min. damping per length	6.9 dB/m	10.2 dB/m

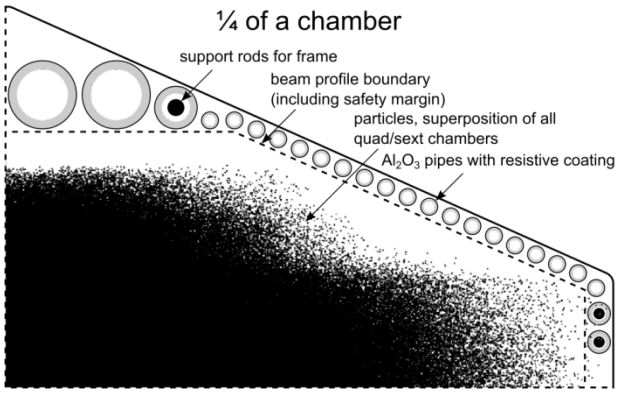

Figure 8: Topography of beam and tubes inside the hexagonal quadrupole/sextupole chamber.

The damping of microwave modes inside the magnet chambers has been simulated (HFSS) with 4 x 24 resistively coated Al_2O_3 tubes (4 diameters from 6 to 24 mm). The result is shown in Fig. 9. The non-dotted lines present the dangerous TM-modes, whose electrical field has the same direction as kicker/pickup field whereas the dashed lines represent the less dangerous TE-modes. A sheet

resistance of R_{sq} = 150 Ω/square +/- 30% has been chosen for sufficient damping of all modes.

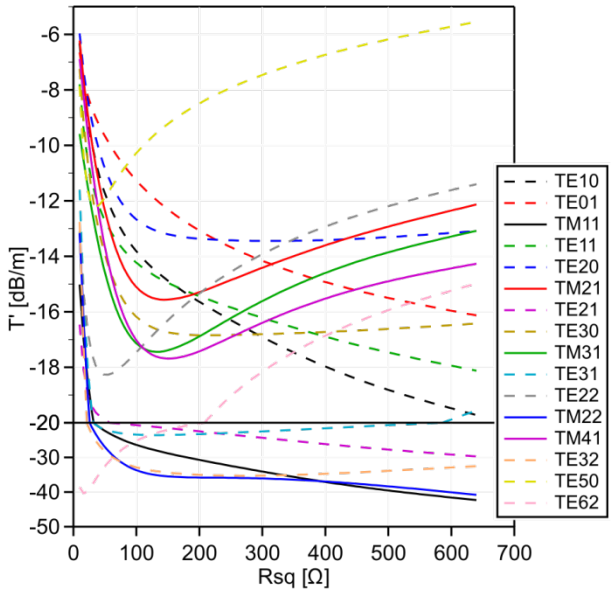

Figure 9: Dependence of damping on sheet resistance.

Ferrites are suitable damping materials inside the pickup and kicker tanks. First, the microwave damping of various ferrite samples was checked by putting them on a microstrip line and measuring the insertion loss. The attenuation corrected by the properties of the microstrip line without ferrite was sufficient in the 1-3 GHz band for all ferrites.

Second, the static specific resistance ρ was measured by contacting planes with a precise Ω-meter. The expected discharging time is given by multiplication with the dielectric constant $\varepsilon_r \cdot \varepsilon_0$ (ε_r=12.9). Acceptable values below 1 ms lie below the red line in Fig. 7.

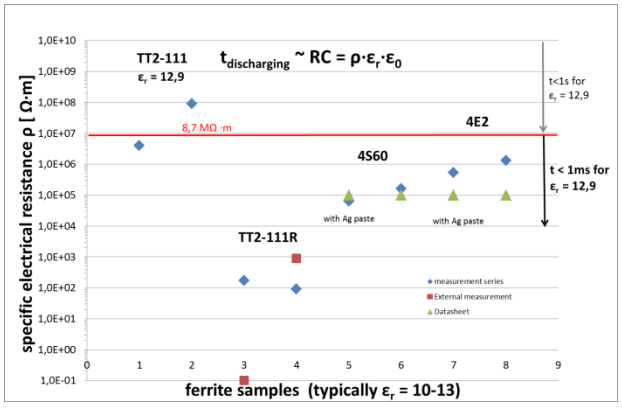

Figure 7: Specific electrical resistance of tested ferrites. The min. and max. values for TT2-111R at room temperature (red squares) are from [2].

The ferrites TT2-111R (Transtech) and 4S60 (Ferroxcube) have been approved for the desired damping of more than 130 dB inside the pickup and kicker tanks. Their outgassing rate was measured and found UHV-acceptable: 2-3 times that of stainless steel (< $1.6 \cdot 10^{-10}$ mbar · l/s ·cm² after 1 week of pumping without bake out).

SIMULATIONS OF THE STOCHASTIC COOLING PROCESS IN THE CR

Simulations of antiproton cooling performance for the most critical case (10^8 protons at 3 GeV, cooling for 10 s all 3 phase-space planes) are shown in Fig. 10. The cooling performance is close to the design limits of the HESR downstream the CR. This is already achieved without plunging the electrodes in these simulations, so there is some margin. The power requirements however are not relaxed since they depend on the initially hot beams.

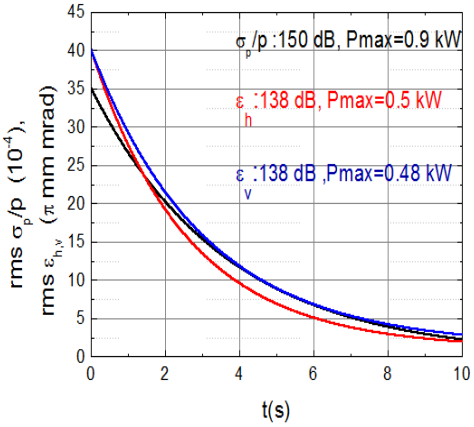

Figure 10: Evolution of rms parameters of the antiproton beam for simultaneous cooling in all 3 planes. P_{max} is the initial cw power at the kicker within the 1-2 GHz band. Four times this value (i.e. to account for statistical beam signal fluctuations) is just within the installed microwave power of 8 kW (power amplifiers at kickers).

REFERENCES

[1] F. Caspers., "Experience with UHV-compatible microwave absorbing materials at CERN", CERN, Geneva, Switzerland, Rep. CERN/PS 1993-10, Feb. 1993.

[2] E. Chojnacki *et al.*, "DC Conductivity of RF absorbing materials", in *Proc. SRF'09*, Berlin, Germany, September 2009, paper THPPO035, pp. 643.